Supporting Information for

Structural Investigation on the Efficient Capture of Cs^+ and Sr^{2+} by a Microporous Cd-Sn-Se Ion Exchanger Constructed from Mono-Lacunary Supertetrahedral Clusters

Jia-Ying Zhu,[†a] Lin Cheng,[†b] Yi-Ming Zhao,[a] Meng-Yu Li,[a] Zi-Zhao Wang,[a] Juan Wang,[a] Cheng Wang,[a] Kai-Yao Wang,*[a]

[a]Tianjin Key Laboratory of Advanced Functional Porous Materials, Institute for New Energy Materials and Low-Carbon Technologies, School of Materials Science and Engineering, Tianjin University of Technology, Tianjin 300384, P. R. China.

[b]College of Chemistry, Tianjin Normal University, Tianjin 300387, P. R. China.

*Corresponding Author: Kai-Yao Wang. Email: kaiyao0729@163.com.

Supporting Information Contents:

Number of pages: 29 (Section S1 to S8).

Number of Figures: 19 (Figure S1 to Figure S19).

Number of Tables: 14 (Table S1 to Table S14).

Section S1. Crystallography and Structural Description.

Table S1. Crystal data for **CdSnSe-1**, **CdSnSe-1Cs** and **CdSnSe-1Sr**.

Compound	**CdSnSe-1**	**CdSnSe-1Cs**	**CdSnSe-1Sr**
Empirical formula	$(CH_3NH_3)_3(NH_4)_3$ $Cd_4Sn_3Se_{13}\cdot(H_2O)_3$	$Cs_{5.6}(CH_3NH_3)_{0.2}(NH_4)_{0.2}$ $Cd_4Sn_3Se_{13}\cdot3.5H_2O$	$Sr_{2.85}(CH_3NH_3)_{0.15}(NH_4)_{0.15}$ $Cd_4Sn_3Se_{13}\cdot6.5H_2O$
Formula weight	2036.53	2649.52	2206.49
Crystal system	Trigonal	Trigonal	Trigonal
Space group	*R*3*m*	*R*3*m*	*R*3*m*
T/K	293(2) K	293(2) K	293(2) K
λ/Å	1.54178	1.54178	1.54178
a/Å	14.94000(10)	14.9443(2)	14.7181(2)
b/Å	14.94000(10)	14.9443(2)	14.7181(2)
c/Å	16.0233(2)	16.4222(4)	16.3882(4)
α/°	90	90	90
β/°	90	90	90
γ/°	120	120	120
V/Å^3	3097.30(6)	3176.24(11)	3074.43(11)
Z	3	3	3
D_c/Mg m^{-3}	3.275	4.156	3.575
μ/mm^{-1}	43.639	79.477	48.533
F(000)	2712	3399	2885
Measured refls.	3943	3666	3905
Independent refls.	1275	1430	1185
R_{int}	0.0388	0.0328	0.0336
No. of parameters	65	62	70
GOF	1.021	1.018	1.025
R_1,[a] wR_2 [$I > 2\sigma(I)$]	0.0356, 0.0952	0.0307, 0.0804	0.0443, 0.1245
R_1, wR_2 (all data)	0.0358, 0.0953	0.0310, 0.0806	0.0447, 0.1260
CCDC	2133519	2133520	2133521

[a] $R_1 = \sum||Fo|-|Fc||/\sum|Fo|$, $wR_2 = \{\sum w[(Fo)^2 -(Fc)^2]^2/\sum w[(Fo)^2]^2\}^{1/2}$

Table S2. Crystal data for **CdSnSe-1Cs-K** and **CdSnSe-1Sr-K**.

Compound	**CdSnSe-1Cs-K**	**CdSnSe-1Sr-K**
Empirical formula	$K_6Cd4Sn_3Se_{13}\cdot 5H_2O$	$Sr_{0.35}K_{5.3}Cd_4Sn_3Se_{13}\cdot 6.5H_2O$
Formula weight	2156.83	2187.15
Crystal system	Trigonal	Trigonal
Space group	*R*3*m*	*R*3*m*
T/K	293(2) K	293(2) K
λ/Å	1.54178	1.54178
a/Å	14.8258(2)	14.8189(2)
b/Å	14.8258(2)	14.8189(2)
c/Å	16.0744(4)	16.0559(4)
α/°	90	90
β/°	90	90
γ/°	120	120
V/Å^3	3059.86(11)	3053.5(2)
Z	3	3
D_c/Mg·m^{-3}	3.511	3.568
μ/mm^{-1}	49.632	49.702
F(000)	2844	2889
Measured refls.	3771	3674
Independent refls.	1410	1374
R_{int}	0.0362	0.0407
No. of parameters	64	58
GOF	1.007	1.003
R_1,[a] wR_2 [$I > 2\sigma(I)$]	0.0357, 0.0912	0.0384, 0.1030
R_1, wR_2 (all data)	0.0363, 0.0916	0.0394, 0.1039
CCDC	2133522	2133523

[a] $R_1 = \sum||Fo|-|Fc||/\sum|Fo|$, $wR_2 = \{\sum w[(Fo)^2 -(Fc)^2]^2/\sum w[(Fo)^2]^2\}^{1/2}$

Table S3. Selected hydrogen-bonding data for **CdSnSe-1**.

D–H···A	*d*(D–H)	*d*(H···A)	*d*(D···A)	<(DHA)
N(1)–H(1D)···Se(2)#1	0.90	2.83	3.52(2)	133.9
N(1)–H(1E)···Se(2)	0.89	2.82	3.52(2)	136.8
N(1)–H(1F)···Se(4)#1	0.90	2.94	3.71(2)	145.2
N(1)–H(1F)···Se(4)#3	0.90	3.13	3.71(2)	124.2
N(2)–H(2D)···Se(3)	0.90	2.63	3.528(19)	179.7
N(2)–H(2A)···O(1W)	0.90	2.07	2.78(4)	135.2
N(2)–H(2B)···Se(3)#2	0.90	3.01	3.528(19)	118.4
N(2)–H(2B)···Se(4)#9	0.90	3.08	3.959(16)	164.7
N(2)–H(2C)···Se(4)#1	0.90	2.88	3.71(2)	152.8
O(1W)–H(1WB)···Se(2)#10	0.85	2.88	3.55(2)	137.0

Symmetry codes: #1 -*x*+3, *y*, -*z*-1/2; #2 -*x*+5/2, -*y*+1/2, -*z*-1; #3 -*x*+3, -*y*, -*z*-1; #4 -*x*+5/2, *y*-1/2, -*z*-1/2; #5 *x*, -*y*, *z*+1/2.

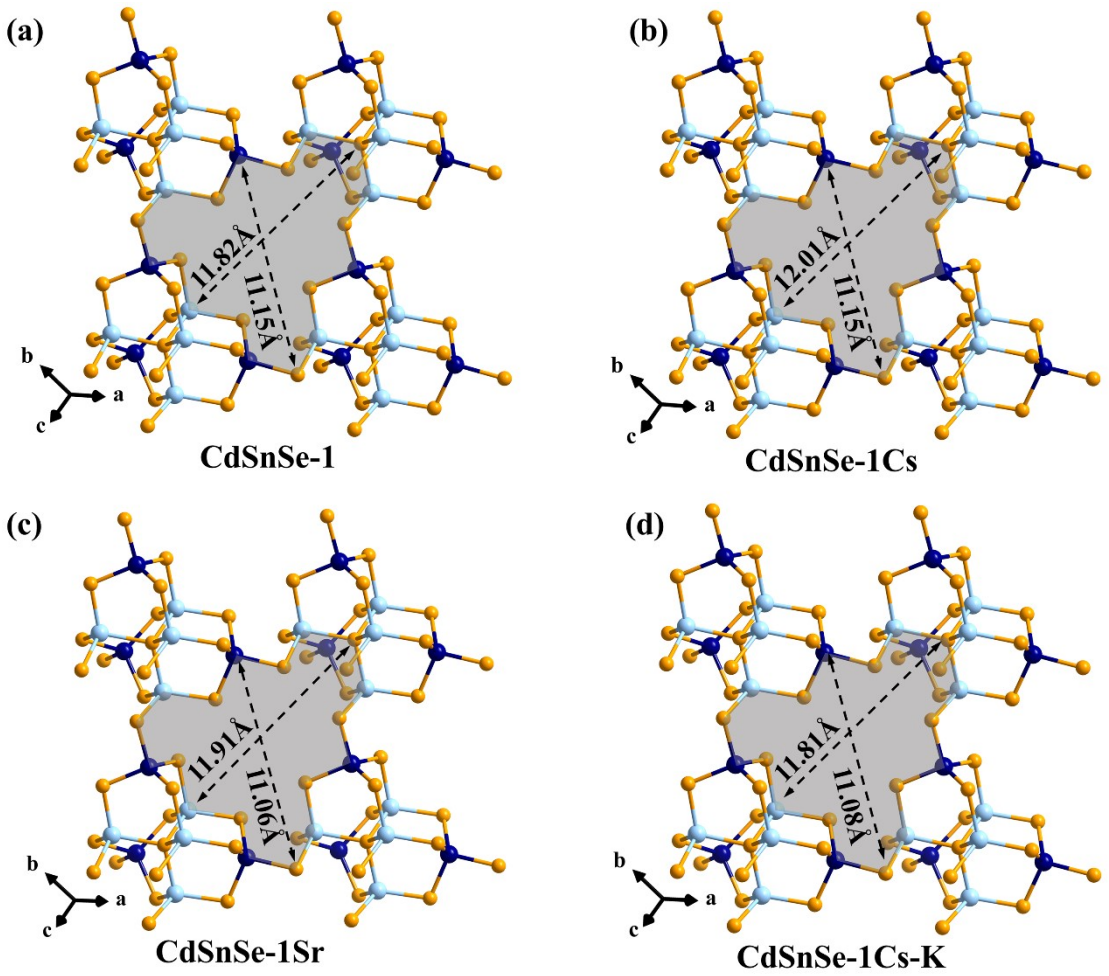

Figure S1. Dimensions of the $\{Cd_5Sn_4Se_9\}$ window (highlighted in grey) in **CdSnSe-1**, **CdSnSe-1Cs**, **CdSnSe-1Sr**, and **CdSnSe-1Cs-K**.

Section S2. Characterizations on the Exchange-Saturated Products.

Table S4. N, C, H elemental analysis on the pristine and exchange-saturated products.

Products	N%	C%	H%
CdSnSe-1	4.151	1.791	1.980
CdSnSe-1Cs	0.096	0.216	0.927
CdSnSe-1Sr	0.182	0.118	1.331
CdSnSe-1Cs-K	0	0	1.138
CdSnSe-1Sr-K	0	0	1.078

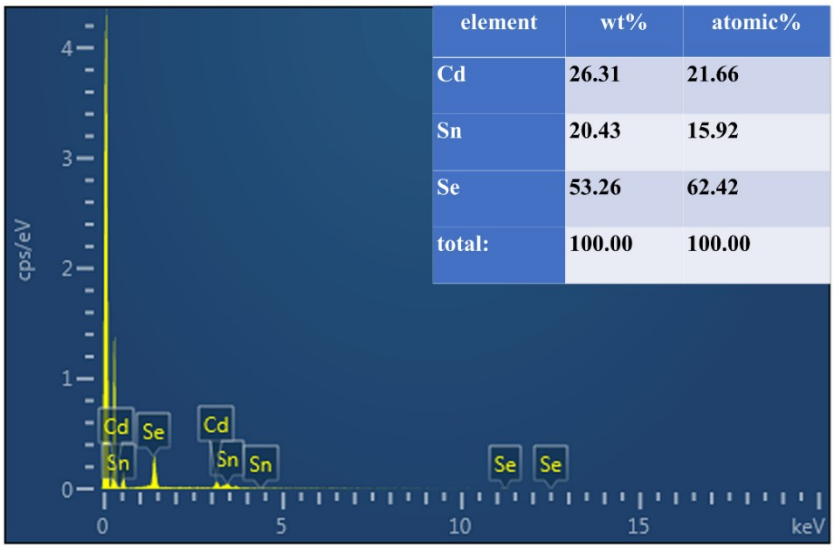

Figure S2. EDS analysis on **CdSnSe-1**.

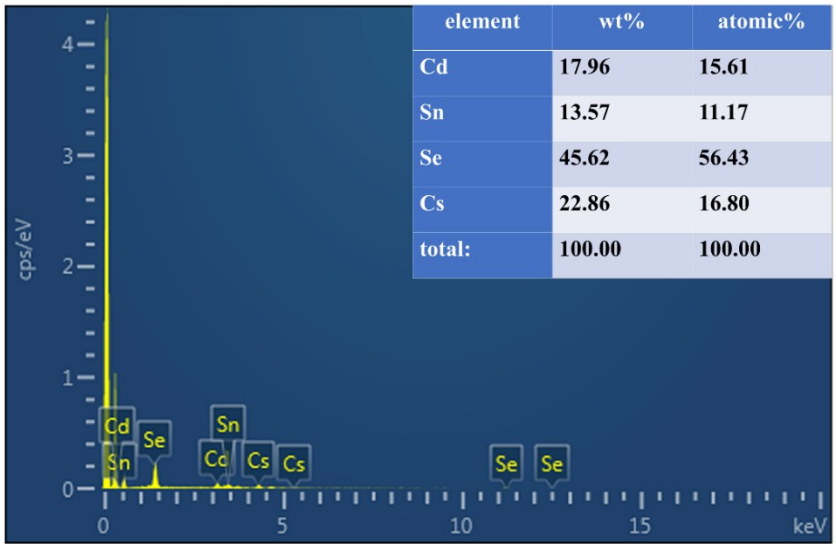

Figure S3. EDS analysis on **CdSnSe-1Cs**.

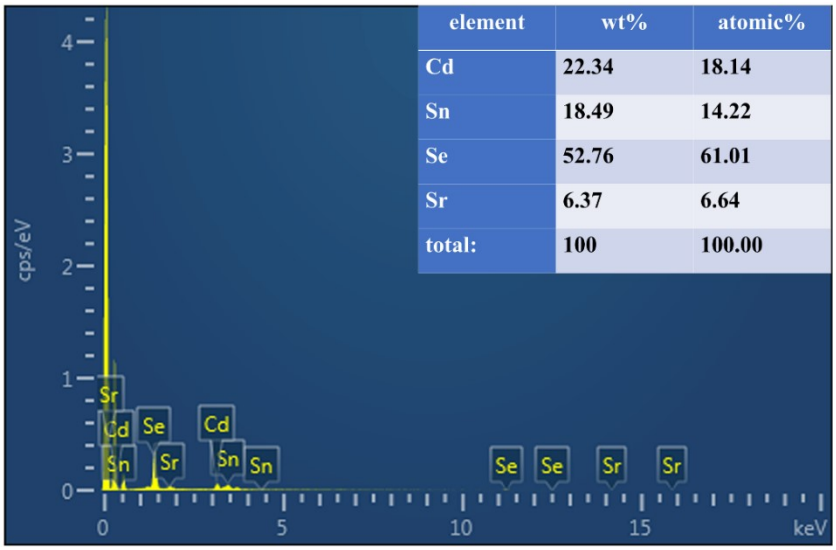

Figure S4. EDS analysis on **CdSnSe-1Sr**.

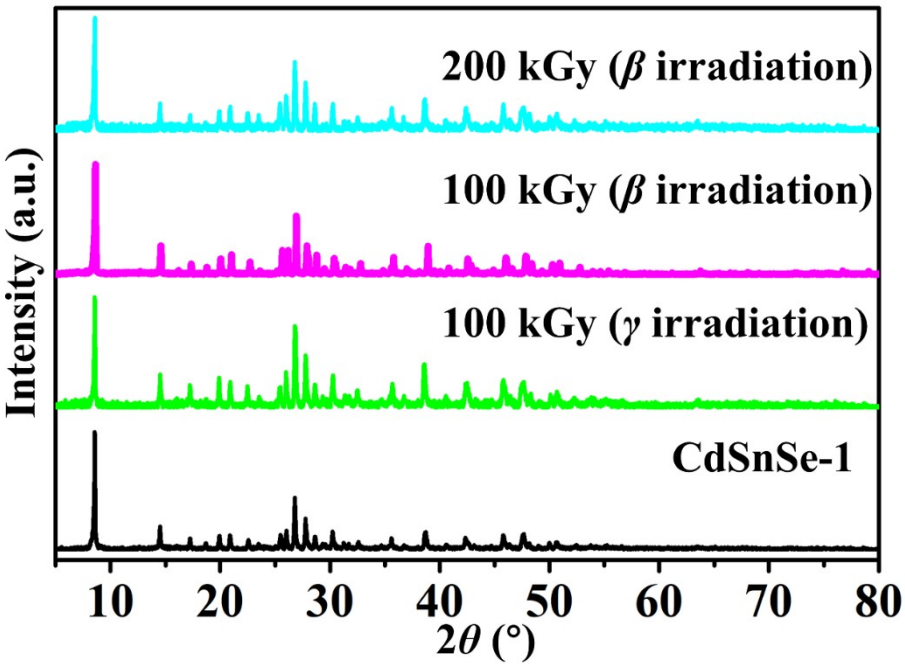

Figure S5. Powder XRD patterns of **CdSnSe-1** before and after β and γ irradiations.

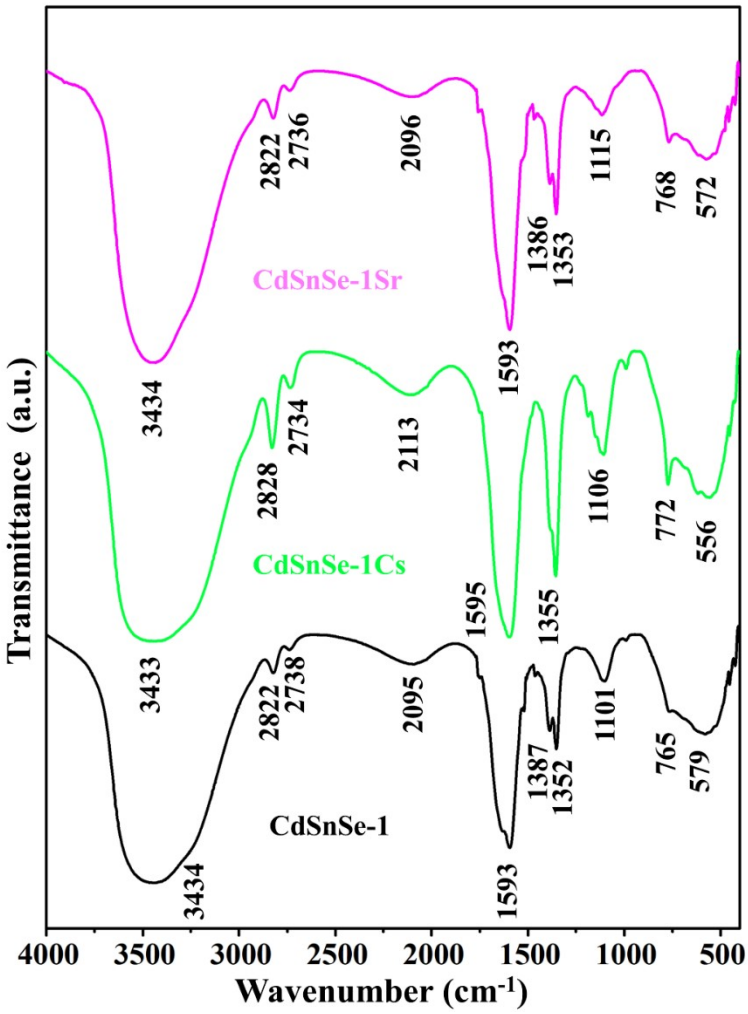

Figure S6. FTIR spectra of **CdSnSe-1**, **CdSnSe-1Cs** and **CdSnSe-1Sr** measured at room temperature on KBr pellets.

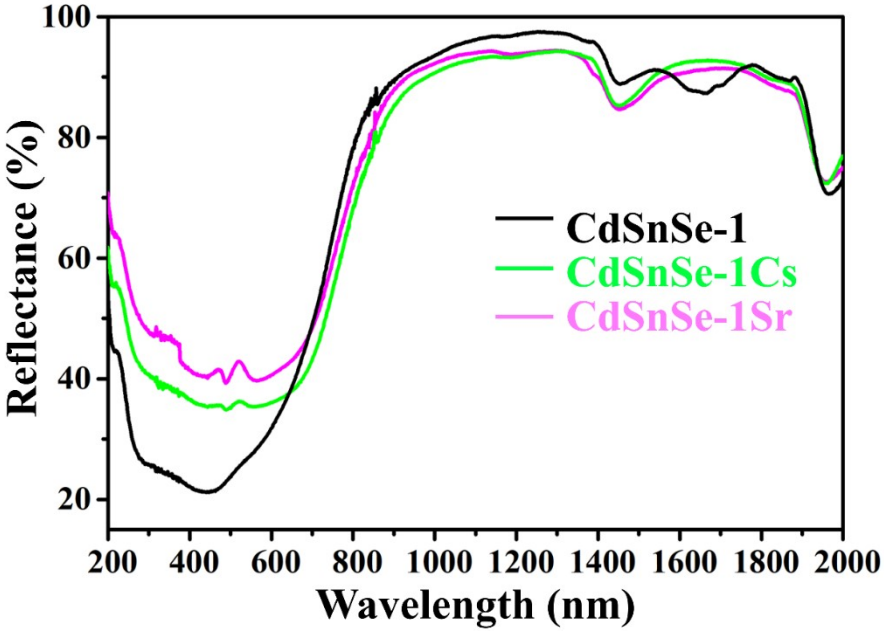

Figure S7. UV/vis reflectance spectra of **CdSnSe-1**, **CdSnSe-1Cs** and **CdSnSe-1Sr**.

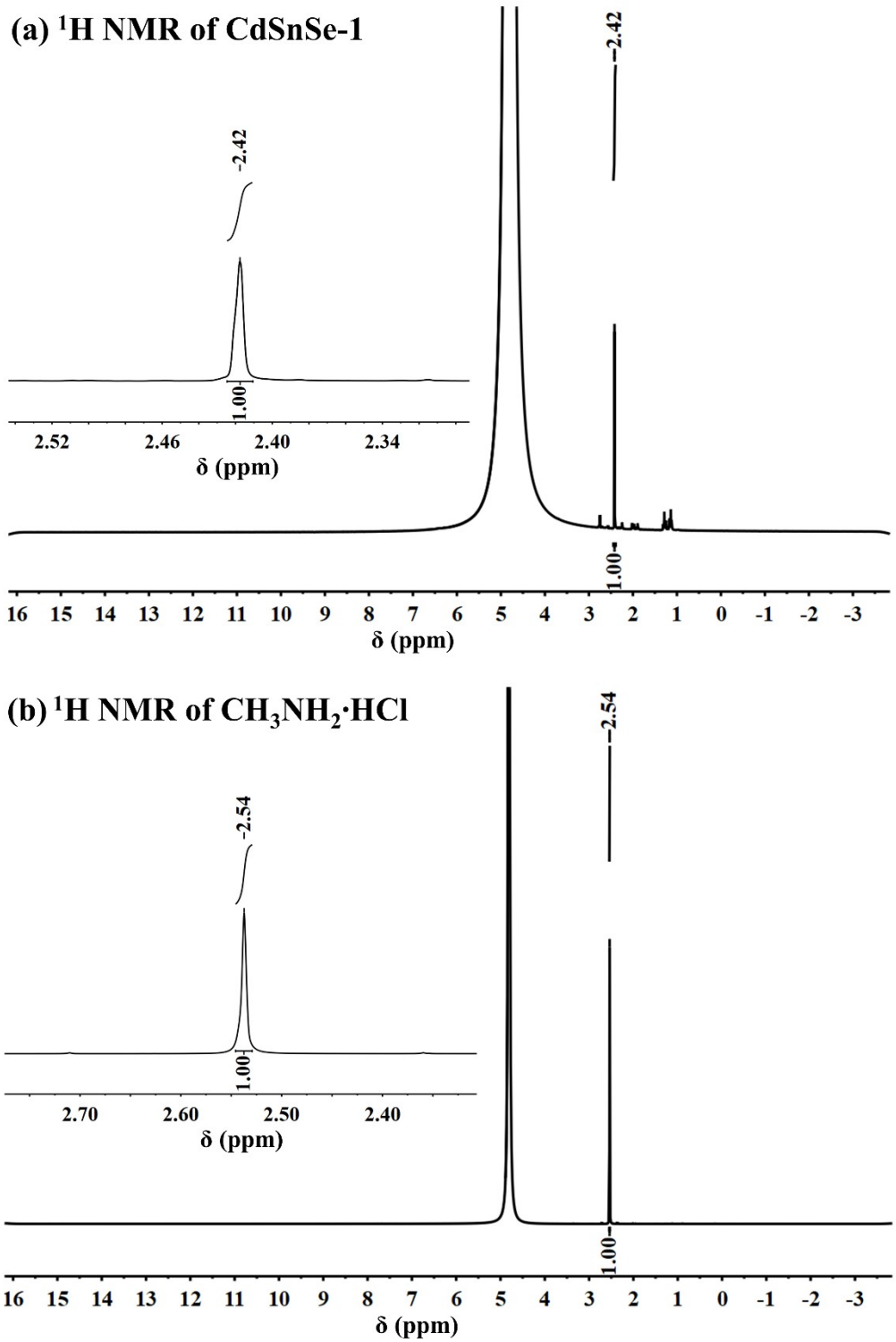

Figure S8. ^{1}H NMR spectra of (a) **CdSnSe-1** and (b) methylamine hydrochloride dissolved in mixed $N_2H_4 \cdot H_2O$ (98%)/D_2O recorded at room temperature.

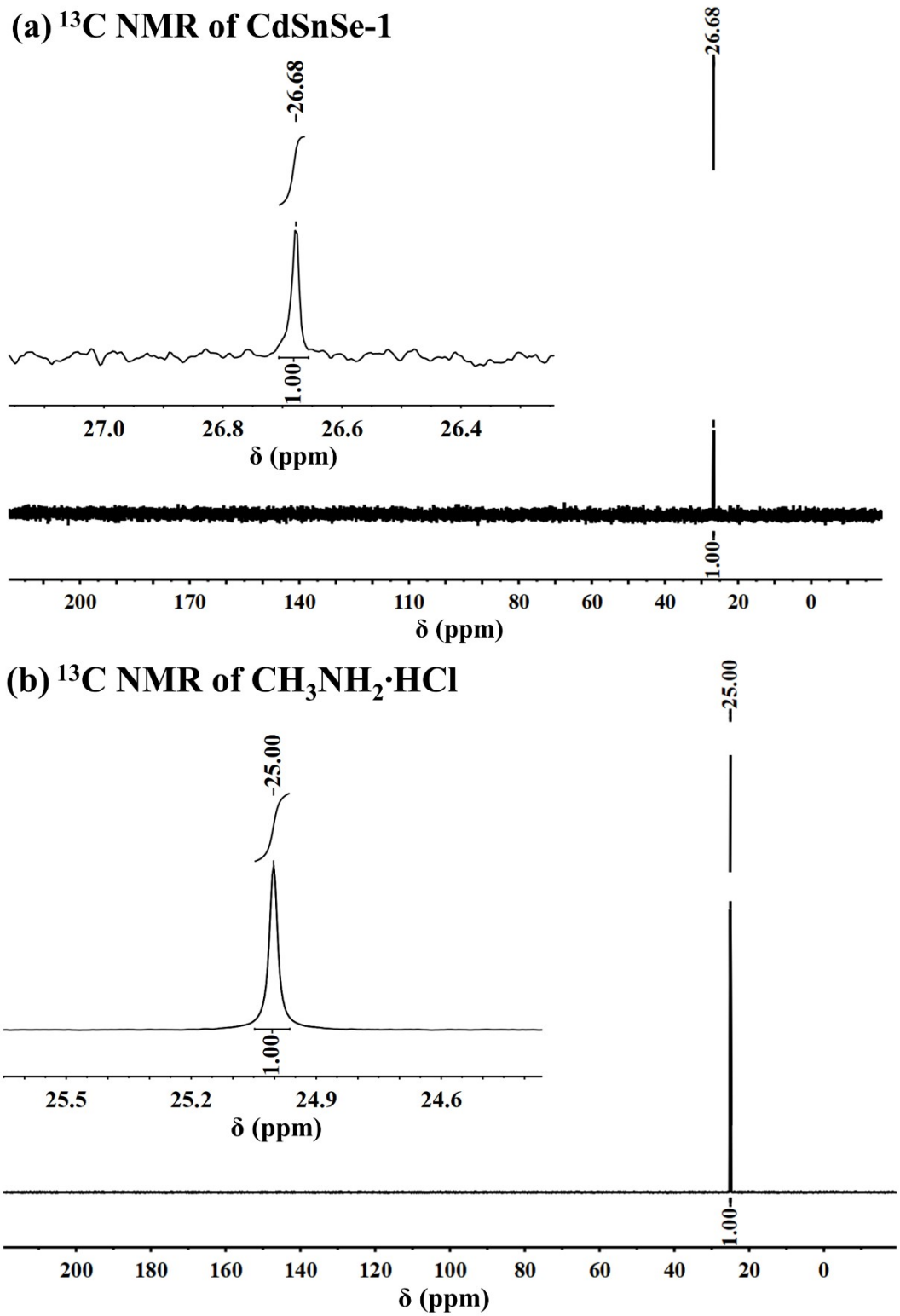

Figure S9. ^{13}C NMR spectra of (a) **CdSnSe-1** and (b) methylamine dissolved in mixed $N_2H_4 \cdot H_2O$ (98%)/D_2O recorded at room temperature.

Section S3. Ion Exchange Kinetics and Isotherms.

Table S5. The parameters calculated for pseudo-second-order kinetic model.

ions	$q_{e,exp}$ (mg g^{-1}, 48 h)	$q_{e,cal}$ (mg g^{-1})	k_2 (g mg^{-1}min^{-1})	R^2
CdSnSe-1				
Cs^+	5.61	5.79	0.00212	0.99982
Sr^{2+}	5.75	5.85	0.00373	0.99922
CdSnSe-1Cs-K				
Cs^+	5.70	5.88	0.00240	0.99870
Sr^{2+}	5.64	5.99	0.00100	0.99790

Table S6. The parameters calculated for Langmuir and Langmuir-Freundlich models applied for Cs^+ and Sr^{2+} ion exchange isotherm fitting.

Model	q_m (mg g^{-1})	b (L mg^{-1})	n	R^2
Cs^+				
Langmuir	371.377 ± 31.52	0.0044 ± 0.0009	—	0.99197
Sr^{2+}				
Langmuir-Freundlich	128.40 ± 60.34	0.0015 ± 0.0033	2.415 ± 0.563	0.98002

Table S7. Comparison between the individual Cs^+ and Sr^{2+} ion exchange capacities of **CdSnSe-1** and those of other exchangers.

Adsorbents	**Ions**	q_m **(mg g^{-1})**	**Ref.**
AMP-PAN	Cs^+	80.1	[1]
	Sr^{2+}	15.8	
Phl	Cs^+	22.5	[2]
	Sr^{2+}	14.9	
PMM	Cs^+	93.3	[3]
	Sr^{2+}	12.5	
NaMT1	Cs^+	290.7	[4]
	Sr^{2+}	184.8	
HKUST-1	Cs^+	153	[5]
CBCA@STS	Cs^+	195.4	[6]
TAM-5	Cs^+	191.8	[7]
I-as	Cs^+	134	[8]
$Na_2V_6O_{16}\cdot 3H_2O$	Cs^+	284	[9]
	Sr^{2+}	96.4	
Zeolite A	Cs^+	207.5	[10]
	Sr^{2+}	303	
LitoFill	Cs^+	54.5	[11]
	Sr^{2+}	30	
AO-XZ	Cs^+	222.2	[12]
Clay	Cs^+	46.3	[13]
	Sr^{2+}	39.7	
FJSM-InMOF	Cs^+	198.6	[14]
	Sr^{2+}	43.8	
FJSM-CA	Sr^{2+}	21.3	[15]
SZ-7	Sr^{2+}	183	[16]
CST	Sr^{2+}	33.9	[17]
SZ-4	Sr^{2+}	117.9	[18]
AMPA-GO	Sr^{2+}	142.4	[19]
SZ-6	Sr^{2+}	61.4	[20]
SZ-5	Sr^{2+}	118.6	[21]
MnO_2-PMMA	Sr^{2+}	49.1	[22]

Table S8. Summary of the Cs^+, Sr^{2+} ion exchange capacities for metal sulfides.

Adsorbents	Ions	q_m (mg g^{-1})	Ref
$K_{2x}Mn_xSn3_{-x}S_6$ (KMS-1, x = 0.5-0.95)	Cs^+	226	[23, 24]
	Sr^{2+}	77	
$K_{2x}Mg_xSn3_{-x}S_6$ (KMS-2, x = 0.5-1)	Cs^+	531.7	[25]
	Sr^{2+}	86.89	
$K_{2x}Sn_{4-x}S_{8-x}$ (KTS-3, x = 0.65-1)	Cs^+	280	[26]
	Sr^{2+}	102	
$K_2Sn_4S_9$ (KTS-1)	Cs^+	205	[27]
$[In_{10.5}S_{14.5}][(H_2NCH_2CH_2NHCH_2)_2]_{2.5}$	Cs^+	41.23	[28]
	Sr^{2+}	62.2	
$(Me_2NH_2)_{1.33}(Me_3NH)_{0.67}Sn_3S_7\cdot 1.25H_2O$ (FJSM-SnS)	Cs^+	408.91	[29]
	Sr^{2+}	65.19	
$[CH_3NH_3][Bmmim]Sn_3S_7\cdot 0.5H_2O$ (FJSM-SnS-2)	Cs^+	266.54	[30]
	Sr^{2+}	59.41	
$[CH_3NH_3]_{0.75}[Bmmim]_{1.25}Sn_3S_7\cdot H_2O$ (FJSM-SnS-3)	Cs^+	109.68	
	Sr^{2+}	57.81	
$[Me_2NH_2]_2[Ga_2Sb_2S_7]\cdot H_2O$ (FJSM-GAS-1)	Cs^+	164	[31]
	Sr^{2+}	80	
$[CH_3NH_3]_{20}Ge_{10}Sb_{28}S_{72}\cdot 7H_2O$	Cs^+	230.91	[32]
$[MeNH_3]_3Sb_9S_{15}$ (FJSM-SbS)	Cs^+	143.47	[33]
$K_{1.87}ZnSn_{1.68}S_{5.30}$ (KZTS)	Sr^{2+}	19.3	[34]
NaZTS	Sr^{2+}	40.4	[35]
KZTS-NS	Sr^{2+}	55.7	[36]
$Na_2Sn_2S_7$ (NaTS)	Sr^{2+}	80	[37]
$(Heta)_{9.5}(H_3O)_{2.5}[In_8Sn_{12}O_{10}S_{32}]\cdot 22H_2O$	Cs^+	537.7	[38]
K@RWY	Cs^+	316	[39]
$Na_5Zn_{3.5}Sn_{3.5}S_{13}\cdot 6H_2O$ (ZnSnS-1)	Sr^{2+}	124.2	[40]
$[CH_3CH_2NH_3]_6In_6S_{12}$ (InS-1)	Sr^{2+}	105.35	[41]
$[CH_3CH_2NH_3]_6In_8S_{15}$ (InS-2)	Sr^{2+}	143.29	[42]
$[NH_3CH_3]_{0.75}Cu_{1.25}GeSe_3$ (CuGeSe-1)	Cs^+	225.3	[43]
$[NH_3CH_3]_{0.5}[NH_2(CH_3)_2]_{0.25}Ag_{1.25}SnSe_3$ (AgSnSe-1)	Cs^+	174.4	[44]
FJSM-SnS-4	Cs^+	388.94	[45]
FJSM-SnS-4	Sr^{2+}	141.22	
KATS-2	Cs^+	358	[46]

Section S4. Elution.

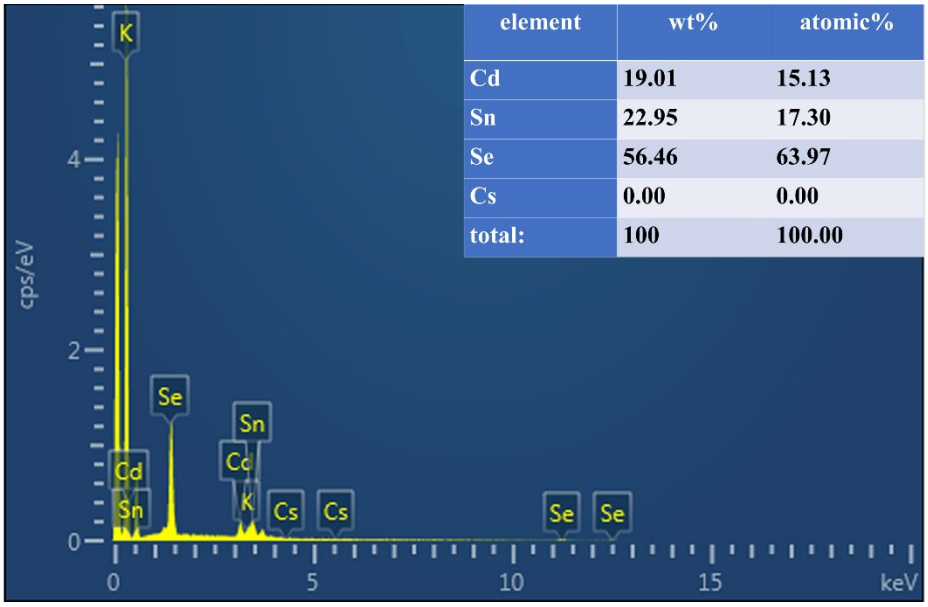

element	wt%	atomic%
Cd	19.01	15.13
Sn	22.95	17.30
Se	56.46	63.97
Cs	0.00	0.00
total:	100	100.00

Figure S10. EDS analysis on the eluted product **CdSnSe-1Cs-K**.

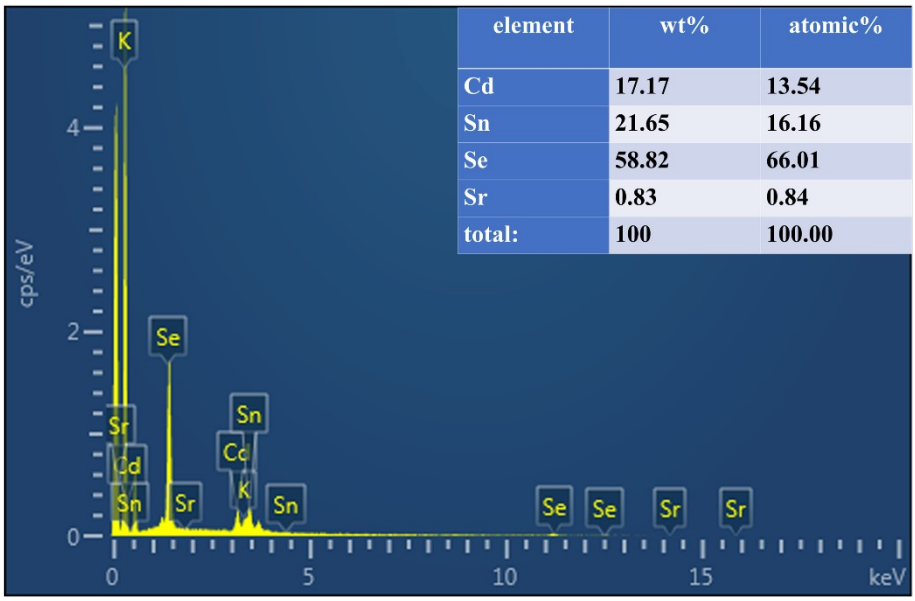

element	wt%	atomic%
Cd	17.17	13.54
Sn	21.65	16.16
Se	58.82	66.01
Sr	0.83	0.84
total:	100	100.00

Figure S11. EDS analysis on the eluted product **CdSnSe-1Sr-K** .

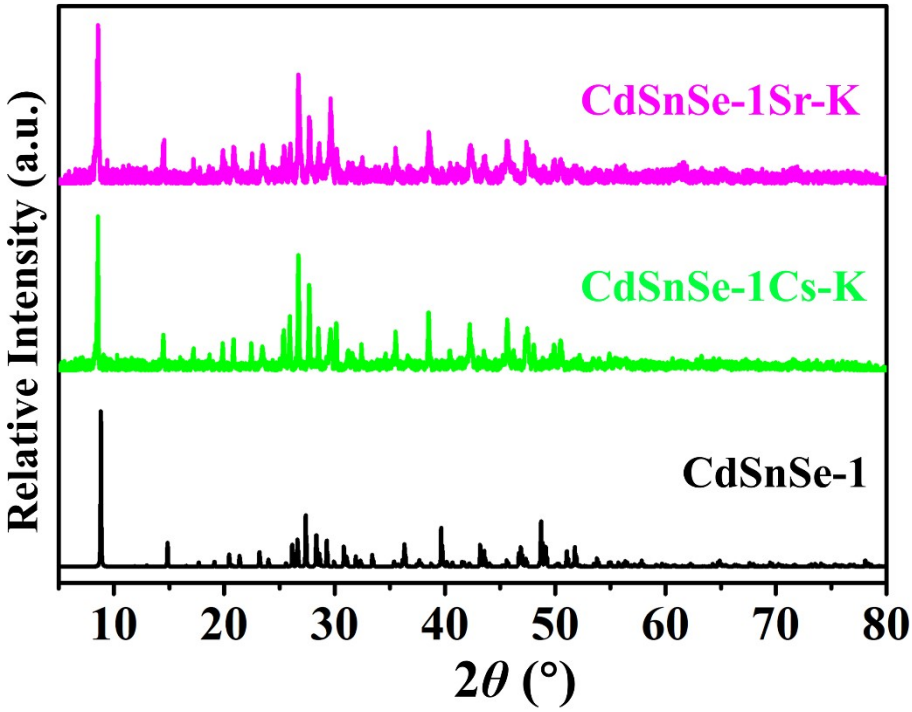

Figure S12. Powder XRD patterns of **CdSnSe-1** and eluted products **CdSnSe-1Cs-K** and **CdSnSe-1Sr-K**.

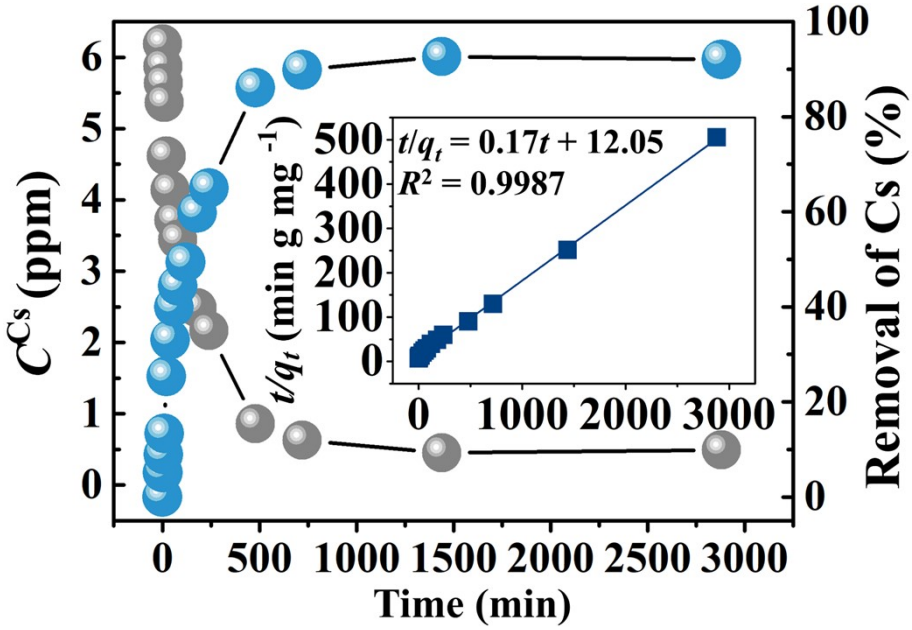

Figure S13. Kinetic curve of Cs^+ ion exchange by **CdSnSe-1Cs-K** (C_0^{Cs} = 6.19 ppm). Inset: plot of t/q_t versus t.

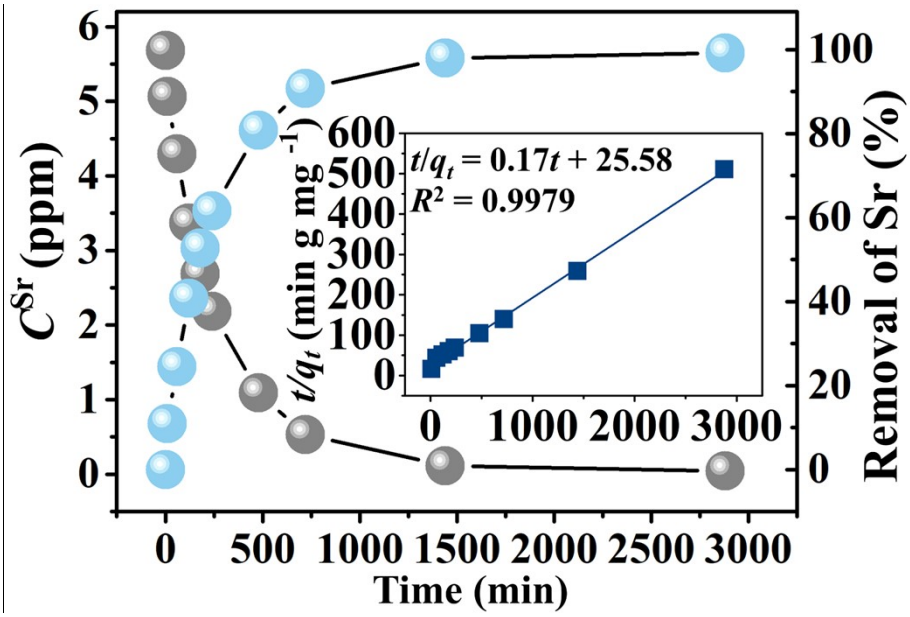

Figure S14. Kinetic curve of Sr^{2+} ion exchange by **CdSnSe-1Sr-K** (C_0^{Sr} = 5.68 ppm). Inset: plot of t/q_t versus t.

Section S5. Structural and Theoretical Investigation on the Ion Exchange.

Table S9. Summary of adsorption energies from theoretical calculation.

Ions	E(fram+ad) /eV mol^{-1}	E(fram) /eV mol^{-1}	E(ad) /eV mol^{-1}	ΔE_{ad} /eV mol^{-1}	ΔE_{ad} /kcal mol^{-1}
Cs^+ (void I)	-64.46	-60.3093	-1.8895	-2.26117	-51.95
Cs^+ (void II)	-80.5227	-76.3787	-1.8895	-2.25449	-51.79
Sr^{2+} (void III)	-57.662	-48.7297	-1.92951	-7.00271	-160.87

Table S10. Weight loss and crystalline water of pristine, exchanged and eluted products.

Products	Weight loss (%) (40-150 °C)	Number of H_2O (per formula)
CdSnSe-1	1.747	3
CdSnSe-1Cs	2.402	3.5
CdSnSe-1Sr	5.381	6.5
CdSnSe-1Cs-K	4.133	5
CdSnSe-1Sr-K	5.376	6.5

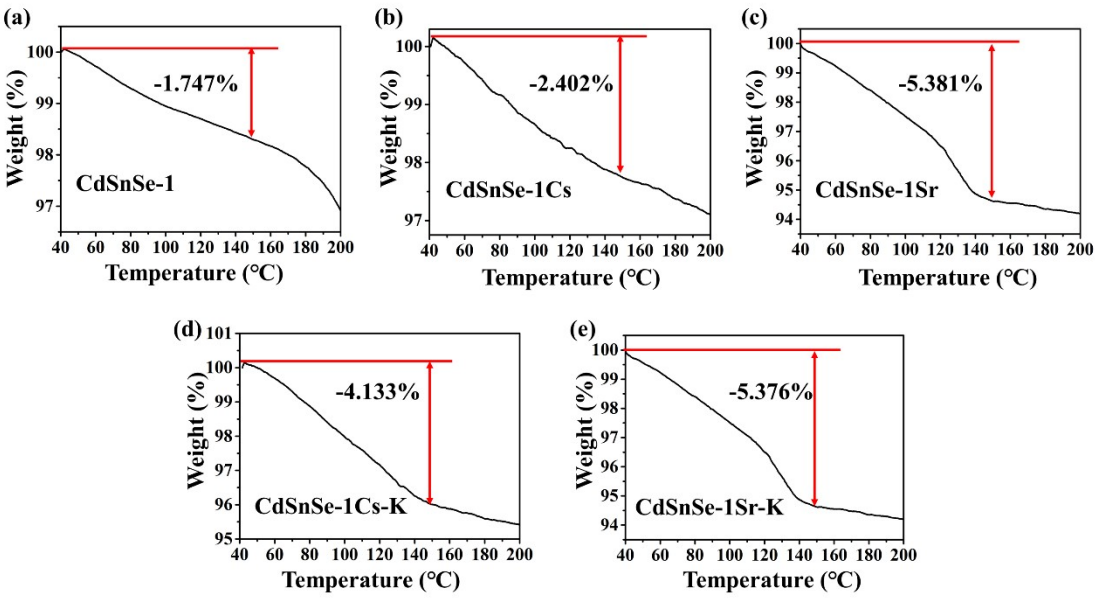

Figure S15. TG curves of the pristine, exchanged and eluted products.

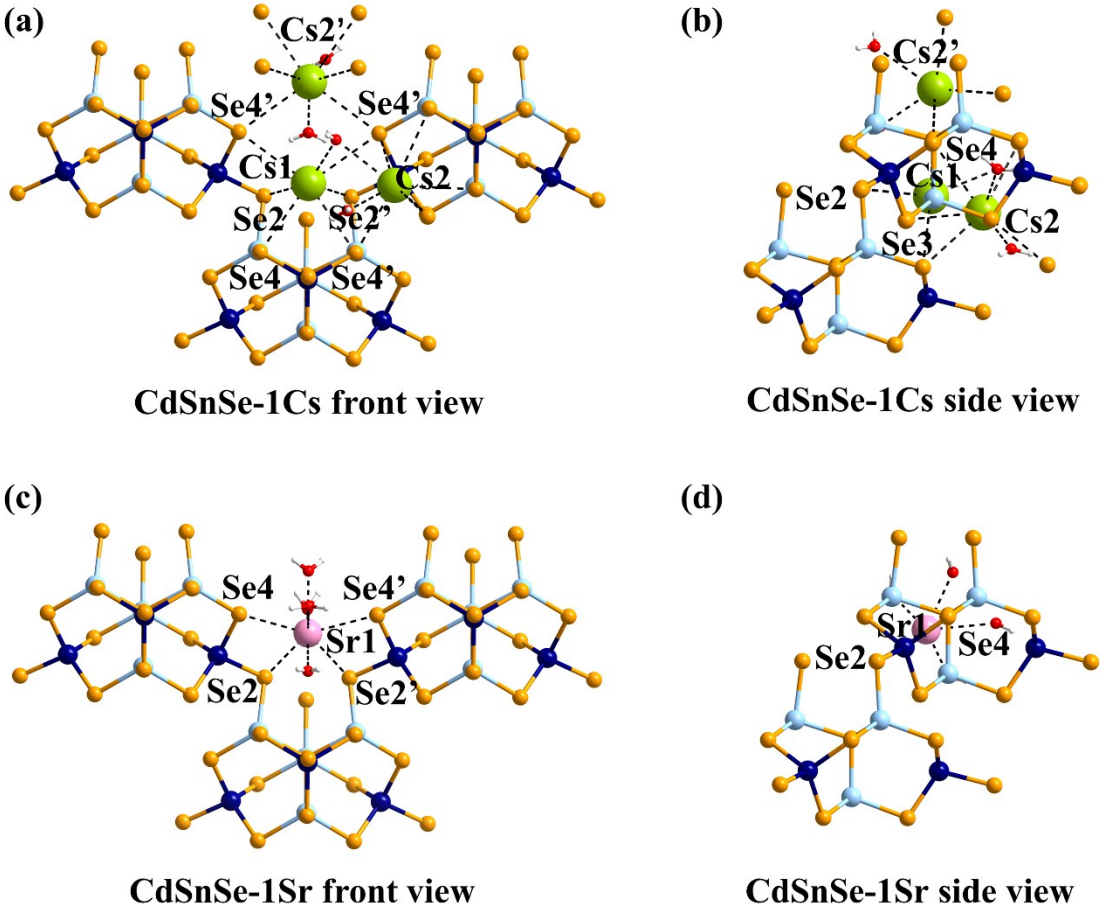

Figure S16. Front and side views of the Cs^{+} and Sr^{2+} location in **CdSnSe-1Cs** and **CdSnSe-1Sr**, respectively.

Section S6. Effect of pH on the Ion Exchange.

Table S11. Removal rates (R) and K_d values of individual Cs^+ and Sr^{2+} using **CdSnSe-1** in pH 0-14 (C_0 ~ 6 ppm; V/m = 1000 mL g^{-1}; room temperature).

pH	R^{Cs} (%)	K_d^{Cs} (mL g^{-1})	R^{Sr} (%)	K_d^{Sr} (mL g^{-1})
0	5.68	60.24995	4.42	46.22164
1	16.80	201.90401	4.40	45.98654
2	31.67	463.38116	35.54	551.32973
3	49.44	977.99591	54.19	1183.05658
4	84.29	5365.39953	88.14	7434.78261
5	91.74	11102.6694	92.09	11642.69142
6	89.80	8804.08654	95.15	19628.93617
7	80.16	4040.57428	78.74	3703.76072
8	81.86	4512.94008	86.51	6411.61707
9	85.70	5991.17737	87.59	7055.87447
10	84.87	5607.82609	91.81	11203.15343
11	93.40	14155.44761	93.75	15002.90065
12	78.33	3614.7875	78.11	3567.51964
13	19.96	249.31888	42.73	746.09248
14	15.96	189.91411	15.94	189.61326

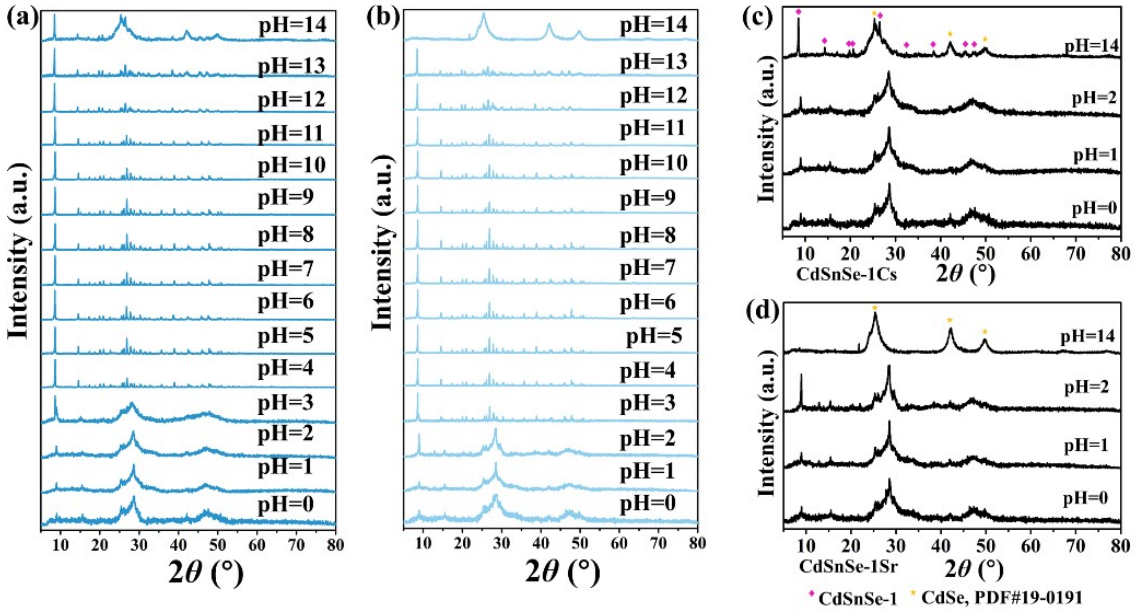

Figure S17. Powder XRD patterns of (a) Cs^{+}- and (b) Sr^{2+}-exchanged products at different pH values. (c,d) Phase identification of the Cs^{+}- and Sr^{2+}-exchanged products at pH 0, 1, 2, 14.

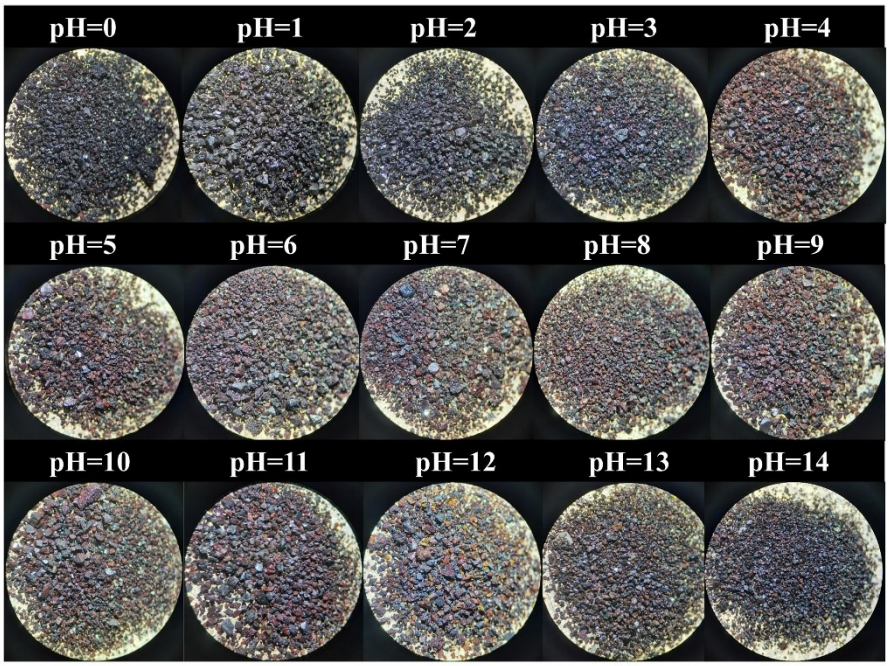

Figure S18. Photographs of the Cs^{+}-exchanged products obtained from the test solutions with pH varying from 0 to 14.

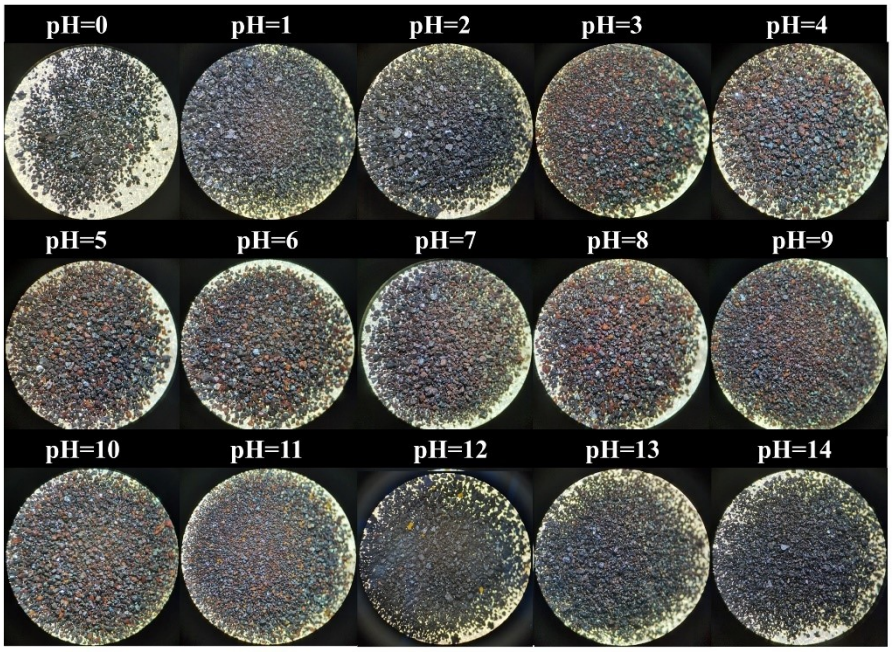

Figure S19. Photographs of the Sr^{2+}-exchanged products obtained from the test solutions with pH varying from 0 to 14.

Section S7. Effect of Coexisting Ions on the Ion Exchange.

Table S12. Removal rates (R) and K_d values for the Cs^+ and Sr^{2+} exchange with increasing concentrations of Na^+, K^+, Mg^{2+} and Ca^{2+} from 0 to 100 mmol L^{-1}.

C (mmol L^{-1})	R^{Cs} (%)	K_d^{Cs} (mL g^{-1})	R^{Sr} (%)	K_d^{Sr} (mL g^{-1})
Na^+				
0	89.80	8804.08654	95.15	19628.93617
0.1	92.36	12090.59233	98.05	50304.24528
1	83.08	4909.03906	98.79	81695.8042
10	82.46	4702.56971	96.21	25409.62289
100	50.75	1030.44008	37.08	589.30163
K^+				
0	89.80	8804.08654	95.15	19628.93617
0.1	91.58	10876.13293	98.91	91121.62162
1	78.84	3726.91754	96.91	31360.84142
10	53.82	1165.41719	95.69	22187.21461
100	21.13	267.85334	46.24	860.03521
Mg^{2+}				
0	89.80	8804.08654	95.15	19628.93617
0.1	84.07	5277.95906	85.07	5698.4625
1	77.47	3438.43594	61.47	1595.55041
10	75.05	3007.63494	41.80	718.17068
100	57.22	1337.4359	38.09	615.36003
Ca^{2+}				
0	89.80	8804.08654	95.15	19628.93617
0.1	87.98	7319.71514	88.76	7897.50329
1	66.15	1954.11196	46.27	861.18044
10	69.53	2281.95545	7.11	76.52745
100	60.20	1512.82633	7.53	81.38239

Section S8. Ion Exchange in Actual Water Environments.

Table S13. The actual pH and concentrations of Na^+, K^+, Mg^{2+} and Ca^{2+} measured in deionized water (DW), mineral water (MW), tap water (TW), and lake water (LW). The water samples were taken from the same sources reported in J. Hazard. Mater. 2022, 425, 128007.[47]

Water	pH	Na^+ (ppm)	K^+ (ppm)	Mg^{2+} (ppm)	Ca^{2+} (ppm)
DW	6.11	0.38	0.30	0.03	NA
MW	7.83	5.31	3.69	4.35	9.88
TW	7.96	6.16	1.81	4.75	36.3
LW	8.27	683.05	25.05	102.80	81.20

Table S14. The removal rates (R) and K_d values for individual Cs^+ and Sr^{2+} ion exchange in DW, MW, TW, and LW. (C_0 ~ 6 ppm; V/m = 1000 mL g^{-1}; room temperature).

Water	R^{Cs} (%)	K_d^{Cs} (mL g^{-1})	R^{Sr} (%)	K_d^{Sr} (mL g^{-1})
DW	89.80	8804.08654	95.15	19628.93617
MW	77.41	3426.66917	47.81	916.14958
TW	79.31	3832.94907	38.83	634.85596
LW	54.62	1203.77358	17.05	205.59507

References:

1. Park, Y.; Lee, Y.-C.; Shin, W. S.; Choi, S.-J., Removal of cobalt, strontium and cesium from radioactive laundry wastewater by ammonium molybdophosphate–polyacrylonitrile (AMP–PAN). *Chem. Eng. J.* **2010,** *162*, 685-695.

2. Tamura, K.; Kogure, T.; Watanabe, Y.; Nagai, C.; Yamada, H., Uptake of Cesium and Strontium Ions by Artificially Altered Phlogopite. *Environ. Sci. Technol.* **2014,** *48*, 5808-5815.

3. Ma, B.; Oh, S.; Shin, W. S.; Choi, S.-J., Removal of Co^{2+}, Sr^{2+} and Cs^{+} from aqueous solution by phosphate-modified montmorillonite (PMM). *Desalination* **2011,** *276*, 336-346.

4. Kim, Y.; Kim, Y. K.; Kim, J. H.; Yim, M.-S.; Harbottle, D.; Lee, J. W., Synthesis of functionalized porous montmorillonite via solid-state NaOH treatment for efficient removal of cesium and strontium ions. *Appl. Surf. Sci.* **2018,** *450*, 404-412.

5. Naeimi, S.; Faghihian, H., Performance of novel adsorbent prepared by magnetic metal-organic framework (MOF) modified by potassium nickel hexacyanoferrate for removal of Cs^{+} from aqueous solution. *Sep. Purif. Technol.* **2017,** *175*, 255-265.

6. Ding, D.; Li, K.; Fang, D.; Ye, X.; Hu, Y.; Tan, X.; Liu, H.; Wu, Z., Novel Biomass-Derived Adsorbents Grafted Sodium Titanium Silicate with High Adsorption Capacity for Rb^{+} and Cs^{+} in the Brine. *ChemistrySelect* **2019,** *4*, 13630-13637.

7. Zheng, Z.; Philip, C. V.; Anthony, R. G.; Krumhansl, J. L.; Trudell, D. E.; Miller, J. E., Ion Exchange of Group I Metals by Hydrous Crystalline Silicotitanates. *Ind. Eng. Chem. Res.* **1996,** *35*, 4246-4256.

8. Seino, S.; Kawahara, R.; Ogasawara, Y.; Mizuno, N.; Uchida, S., Reduction-Induced Highly Selective Uptake of Cesium Ions by an Ionic Crystal Based on Silicododecamolybdate. *Angew. Chem. Int. Edit.* **2016,** *55*, 3987-3991.

9. Sarina, S.; Bo, A.; Liu, D.; Liu, H.; Yang, D.; Zhou, C.; Maes, N.; Komarneni, S.; Zhu, H., Separate or Simultaneous Removal of Radioactive Cations and Anions from Water by Layered Sodium Vanadate-Based Sorbents. *Chem. Mat.* **2014,** *26*, 4788-4795.

10. El-Kamash, A. M., Evaluation of zeolite A for the sorptive removal of Cs^{+} and Sr^{2+} ions from aqueous solutions using batch and fixed bed column operations. *J.*

Hazard. Mater. **2008,** *151*, 432-445.

11. Sterba, J. H.; Sperrer, H.; Wallenko, F.; Welch, J. M., Adsorption characteristics of a clinoptilolite-rich zeolite compound for Sr and Cs. *J. Radioanal. Nucl. Chem.* **2018,** *318*, 267-270.

12. Liao, H.; Li, Y.; Li, H.; Li, B.; Zhou, Y.; Liu, D.; Wang, X., Efficiency and mechanism of amidoxime-modified X-type zeolite (AO-XZ) for Cs^+ adsorption. *Chem. Phys. Lett.* **2020,** *741*, 137084.

13. Abdel-Karim, A.-A. M.; Zaki, A. A.; Elwan, W.; El-Naggar, M. R.; Gouda, M. M., Experimental and modeling investigations of cesium and strontium adsorption onto clay of radioactive waste disposal. *Appl. Clay Sci.* **2016,** *132-133*, 391-401.

14. Gao, Y.-J.; Feng, M.-L.; Zhang, B.; Wu, Z.-F.; Song, Y.; Huang, X.-Y., An easily synthesized microporous framework material for the selective capture of radioactive Cs^+ and Sr^{2+} ions. *J. Mater. Chem. A* **2018,** *6*, 3967-3976.

15. Ma, W.; Hu, B.; Li, J.-L.; Zhang, Z.-Z.; Zeng, X.; Jin, J.; Li, Z.; Zheng, S.-T.; Feng, M.-L.; Huang, X.-Y., The Uptake of Hazardous Metal Ions into a High-Nuclearity Cluster-Based Compound with Structural Transformation and Proton Conduction. *ACS Appl. Mater. Interfaces* **2020,** *12*, 26222-26231.

16. Zhang, J.; Chen, L.; Dai, X.; Chen, L.; Zhai, F.; Yu, W.; Guo, S.; Yang, L.; Chen, L.; Zhang, Y.; He, L.; Chen, C.; Chai, Z.; Wang, S., Efficient Sr-90 removal from highly alkaline solution by an ultrastable crystalline zirconium phosphonate. *Chem. Commun.* **2021,** *57*, 8452-8455.

17. Weerasekara, N. A.; Choo, K.-H.; Choi, S.-J., Metal oxide enhanced microfiltration for the selective removal of Co and Sr ions from nuclear laundry wastewater. *J. Membr. Sci.* **2013,** *447*, 87-95.

18. Zhang, J.; Chen, L.; Dai, X.; Zhu, L.; Xiao, C.; Xu, L.; Zhang, Z.; Alekseev, E. V.; Wang, Y.; Zhang, C.; Zhang, H.; Wang, Y.; Diwu, J.; Chai, Z.; Wang, S., Distinctive Two-Step Intercalation of Sr^{2+} into a Coordination Polymer with Record High ^{90}Sr Uptake Capabilities. *Chem* **2019,** *5*, 977-994.

19. Alamdarlo, F. V.; Solookinejad, G.; Zahakifar, F.; Jalal, M. R.; Jabbari, M., Study of kinetic, thermodynamic, and isotherm of Sr adsorption from aqueous solutions on

graphene oxide (GO) and (aminomethyl)phosphonic acid–graphene oxide (AMPA–GO). *J. Radioanal. Nucl. Chem.* **2021,** *329*, 1033-1043.

20. Li, G.; Ji, G.; Liu, W.; Zhang, J.; Song, L.; Cheng, L.; Wang, X.; Wang, Y.; Liu, J.; Chen, X.; Sun, X.; Diwu, J., A hydrolytically stable anionic layered indium–organic framework for the efficient removal of ^{90}Sr from seawater. *Dalton Trans.* **2019,** *48*, 17858-17863.

21. Zhang, J.; Chen, L.; Gui, D.; Zhang, H.; Zhang, D.; Liu, W.; Huang, G.; Diwu, J.; Chai, Z.; Wang, S., An ingenious one-dimensional zirconium phosphonate with efficient strontium exchange capability and moderate proton conductivity. *Dalton Trans.* **2018,** *47*, 5161-5165.

22. Valsala, T. P.; Joseph, A.; Sonar, N. L.; Sonavane, M. S.; Shah, J. G.; Raj, K.; Venugopal, V., Separation of strontium from low level radioactive waste solutions using hydrous manganese dioxide composite materials. *J. Nucl. Mater.* **2010,** *404*, 138-143.

23. Manos, M. J.; Kanatzidis, M. G., Highly Efficient and Rapid Cs^+ Uptake by the Layered Metal Sulfide $K_{2x}Mn_xSn_{3-x}S_6$ (KMS-1). *J. Am. Chem. Soc.* **2009,** *131*, 6599-6607.

24. Manos, M. J.; Ding, N.; Kanatzidis, M. G., Layered metal sulfides: Exceptionally selective agents for radioactive strontium removal. *Proc. Natl. Acad. Sci. U.S.A.* **2008,** *105*, 3696.

25. Mertz, J. L.; Fard, Z. H.; Malliakas, C. D.; Manos, M. J.; Kanatzidis, M. G., Selective Removal of Cs^+, Sr^{2+}, and Ni^{2+} by $K_{2x}Mg_xSn_{3-x}S_6$ (x = 0.5–1) (KMS-2) Relevant to Nuclear Waste Remediation. *Chem. Mat.* **2013,** *25*, 2116-2127.

26. Sarma, D.; Malliakas, C. D.; Subrahmanyam, K. S.; Islam, S. M.; Kanatzidis, M. G., $K_{2x}Sn_{4-x}S_{8-x}$ (x = 0.65–1): a new metal sulfide for rapid and selective removal of Cs^+, Sr^{2+} and UO_2^{2+} ions. *Chem. Sci.* **2016,** *7*, 1121-1132.

27. Kanatzidis, M. G.; Mertz, J.; Manos, M. J., Chalcogenide Compounds for The Remediation of Nuclear and Heavy Metal Wastes, US Pat., US2011290735-A1, **2011**.

28. Lan, Y.; Su, Z.; Li, X.; Jiang, Z.; Jin, J.; Xie, J.; Li, S., Synthesis of a new microporous indium sulphide and its capabilities to the separation of strontium. *J.*

Radioanal. Nucl. Chem. **2007,** *273*, 99-102.

29. Qi, X.-H.; Du, K.-Z.; Feng, M.-L.; Li, J.-R.; Du, C.-F.; Zhang, B.; Huang, X.-Y., A two-dimensionally microporous thiostannate with superior Cs^+ and Sr^{2+} ion-exchange property. *J. Mater. Chem. A* **2015,** *3*, 5665-5673.

30. Li, W.-A.; Li, J.-R.; Zhang, B.; Sun, H.-Y.; Jin, J.-C.; Huang, X.-Y.; Feng, M.-L., Layered Thiostannates with Distinct Arrangements of Mixed Cations for the Selective Capture of Cs^+, Sr^{2+}, and Eu^{3+} Ions. *ACS Appl. Mater. Interfaces* **2021,** *13*, 10191-10201.

31. Feng, M.-L.; Sarma, D.; Gao, Y.-J.; Qi, X.-H.; Li, W.-A.; Huang, X.-Y.; Kanatzidis, M. G., Efficient Removal of $[UO_2]^{2+}$, Cs^+, and Sr^{2+} Ions by Radiation-Resistant Gallium Thioantimonates. *J. Am. Chem. Soc.* **2018,** *140*, 11133-11140.

32. Zhang, B.; Feng, M.-L.; Cui, H.-H.; Du, C.-F.; Qi, X.-H.; Shen, N.-N.; Huang, X.-Y., Syntheses, Crystal Structures, Ion-Exchange, and Photocatalytic Properties of Two Amine-Directed Ge–Sb–S Compounds. *Inorg. Chem.* **2015,** *54*, 8474-8481.

33. Liao, Y.-Y.; Li, J.-R.; Zhang, B.; Sun, H.-Y.; Ma, W.; Jin, J.-C.; Feng, M.-L.; Huang, X.-Y., Robust and Flexible Thioantimonate Materials for Cs^+ Remediation with Distinctive Structural Transformation: A Clear Insight into the Ion-Exchange Mechanism. *ACS Appl. Mater. Interfaces* **2021,** *13*, 5275-5283.

34. Zhang, M.; Gu, P.; Zhang, Z.; Liu, J.; Dong, L.; Zhang, G., Effective, rapid and selective adsorption of radioactive Sr^{2+} from aqueous solution by a novel metal sulfide adsorbent. *Chem. Eng. J.* **2018,** *351*, 668-677.

35. Zhang, M.; Gu, P.; Yan, S.; Dong, L.; Zhang, G. Na/Zn/Sn/S (NaZTS): Quaternary Metal Sulfide Nanosheets for Efficient Adsorption of Radioactive Strontium Ions. *Chem. Eng. J.* **2020**, *379*, 122227.

36. Zhang, M.; Gu, P.; Yan, S.; Pan, S.; Dong, L.; Zhang, G. A Novel Nanomaterial and Its New Application for Efficient Radioactive Strontium Removal from Tap Water: KZTS-NS Metal Sulfide Adsorbent Versus CTA-F-MF Process. *Chem. Eng. J.* **2020**, *391*, 123486.

37. Zhang, Z.; Gu, P.; Zhang, M.; Yan, S.; Dong, L.; Zhang, G. Synthesis of a Robust Layered Metal Sulfide for Rapid and Effective Removal of Sr^{2+} from Aqueous

Solutions. *Chem. Eng. J.* **2019**, *372*, 1205-1215.

38. Wang, L.; Pei, H.; Sarma, D.; Zhang, X.-M.; MacRenaris, K.; Malliakas, C. D.; Kanatzidis, M. G. Highly Selective Radioactive $^{137}Cs^{+}$ Capture in an Open-Framework Oxysulfide Based on Supertetrahedral Cluster. *Chem. Mater.* **2019**, *31*, 1628-1634.

39. Yang, H.; Luo, M.; Luo, L.; Wang, H.; Hu, D.; Lin, J.; Wang, X.; Wang, Y.; Wang, S.; Bu, X.; Feng, P.; Wu, T. Highly Selective and Rapid Uptake of Radionuclide Cesium Based on Robust Zeolitic Chalcogenide via Stepwise Ion-Exchange Strategy. *Chem. Mater.* **2016**, *28*, 8774-8780.

40. Wang, K.-Y.; Ding, D.; Sun, M.; Cheng, L.; Wang, C. Effective and Rapid Adsorption of Sr^{2+} Ions by a Hydrated Pentasodium Cluster Templated Zinc Thiostannate. *Inorg. Chem.* **2019**, *58*, 10184-10193.

41. Wang, K.-Y.; Sun, M.; Ding, D.; Liu H.-W., Cheng L. Wang C. Di-lacunary $[In_6S_{15}]^{12-}$ Cluster: the Building Block of a Highly Negatively Charged Framework for Superior Sr^{2+} Adsorption Capacities. *Chem. Commun.*, **2020**, *56*, 3409-3412.

42. Sun, M.; Wang, K.-Y.; Ding, D.; Zhu, J.-Y.; Zhao, Y.-M.; Cheng, L.; Wang, C. Removal of Sr^{2+} Ions by a High-Capacity Indium Sulfide Exchanger Containing Permeable Layers with Large Pores. *Inorg. Chem.* **2020**, *59*, 13822-13826.

43. Liu, H.-W.; Wang, K.-Y.; Ding, D.; Sun, M.; Cheng, L.; Wang, C. Deep Eutectic Solvothermal Synthesis of an Open Framework Copper Selenidogermanate with pH-resistant Cs^{+} Ion Exchange Properties. *Chem. Commun.* **2019**, *55*, 13884-13887.

44. Ding, D.; Cheng, L.; Wang, K.-Y.; Liu, H.-W.; Sun, M.; Wang, C. Efficient Cs^{+}–Sr^{2+} Separation over a Microporous Silver Selenidostannate Synthesized in Deep Eutectic Solvent. *Inorg. Chem.* **2020**, *59*, 9638-9647.

45. J. Li, J. Jin, T. Zhang, W. Ma, X. Zeng, H. Sun, M. Cheng, M. Feng, X. Huang, Rapid and Selective Uptake of Cs^{+} and Sr^{2+} Ions by a Layered Thiostannate with Acid–Base and Irradiation Resistances, ACS ES&T Water, **2021**, *1*, 2440-2449.

46. Yang, C.; Cho, K. Rapid and selective removal of Cs^{+} from water by layered potassium antimony thiostannate. *J. Hazard. Mater.* **2021**, *403*, 124105.

47. Zhao, Y.-M.; Sun, M.; Cheng, L.; Wang, K.-Y.; Liu, Y.; Zhu, J.-Y.; Zhang, S.; Wang, C., Efficient removal of Ba^{2+}, Co^{2+} and Ni^{2+} by an ethylammonium-templated

indium sulfide ion exchanger, *J. Hazard. Mater.* **2022**, *425*, 128007.